minerals

MDPI

Article

Application of the Mineralogy and Mineral Chemistry of Carbonates as a Genetic Tool in the Hydrothermal Environment

Javier Carrillo-Rosúa [1,2,*], Salvador Morales-Ruano [2,3], Stephen Roberts [4], Diego Morata [5] and Mauricio Belmar [6]

[1] Departamento de Didáctica de las Ciencias Experimentales, Universidad de Granada, Campus Universitario de Cartuja, 18071 Granada, Spain
[2] Instituto Andaluz de Ciencias de la Tierra, Universidad de Granada—C.S.I.C., Avd. Las Palmeras 4, 18100 Armilla, Spain; smorales@ugr.es
[3] Departamento de Mineralogía y Petrología, Universidad de Granada, Avd. Fuentenueva s/n, 18002 Granada, Spain
[4] National Oceanographic Centre, School of Ocean and Earth Science, University of Southampton, European Way, Southampton SO14 3ZH, UK; steve.roberts@noc.soton.ac.uk
[5] Department of Geology and Andean Geothermal Center of Excellence (CEGA), Facultad de Ciencias Físicas y Matemáticas, Universidad de Chile, Plaza Ercilla 803, Santiago 8370450, Chile; dmorata@ing.uchile.cl
[6] Centro de Mineralogía Avanzada/SGS Minerals S.A., Puerto Madero 130, Parque Industrial Puerto Santiago, Pudahuel 9020000, Chile; mauricio.belmar@sgs.com
* Correspondence: fjcarril@ugr.es

Abstract: The mineralogy and mineral chemistry of carbonates from various hydrothermal deposits, including volcanic-hosted Au-Cu epithermal, "Chilean Manto-type" Cu(-Ag), stratabound Mn, and Ag-Ba vein deposits from Spain and Chile, were investigated. Dolomite-ankerite (±siderite) was found in variable amounts within the epithermal deposits and associated hydrothermal alteration, whereas calcite was found either within barren veins or disseminated within the regional alteration. Calcite is the major gangue phase within the stratabound deposits, which tend to lack dolomite/ankerite and siderite. Carbonates precipitated from hydrothermal ore fluids are typically Mn-rich, up to 3.55 at. % in siderite, 2.27 at. % in dolomite/ankerite, and 1.92 at. % in calcite. In contrast, calcite related to very low-grade metamorphism or regional low-temperature alteration is Mn-poor but sometimes Mg-rich, possibly related to a higher temperature of formation. Chemical zonation was observed in the hydrothermal carbonates, although no unique pattern and chemical evolution was observed. This study suggests that the chemical composition of carbonates, especially the Mn content, could be a useful vector within ore-forming hydrothermal systems, and therefore constitutes a possible tool in geochemical exploration. Furthermore, Mn-poor calcites detected in some deposits are suggested to be linked with a later episode, maybe suggesting a predominance of meteoric waters, being not related to the main ore stage formation, thus avoiding misunderstanding of further isotopic studies.

Keywords: hydrothermal; gangue; Mn; carbonate; Spain; Chile

Citation: Carrillo-Rosúa, J.; Morales-Ruano, S.; Roberts, S.; Morata, D.; Belmar, M. Application of the Mineralogy and Mineral Chemistry of Car-bonates as a Genetic Tool in the Hydrothermal Environment. *Minerals* **2021**, *11*, 822. https://doi.org/10.3390/min11080822

Academic Editor: Panagiotis Voudouris

Received: 16 June 2021
Accepted: 26 July 2021
Published: 29 July 2021

1. Introduction

Carbonates are commonly present as part of the gangue in hydrothermal deposits associated with quartz, phyllosilicates, and barite. Carbonates are a focus of interest to researchers investigating ore-forming systems; fluid inclusion and isotopic data (C, O, Sr, Pb) can give important information on the provenance of hydrothermal fluids (e.g., [1–13]). However, only limited works on the composition of carbonates in ore-forming hydrothermal environments are available (e.g., [6,14–17]). Nevertheless, these authors sug-

gest a possible association of an elevated Mn content in carbonates with ore-forming hydrothermal fluids, and Mn has been used as an index of such activity in whole-rock compositions (e.g., [18,19]). Furthermore, recent works in low-temperature non-ore systems have demonstrated the usefulness of applying a full range of techniques in carbonate study, including elemental analysis of carbonates [20–22]. Here, we systematically characterize the mineralogy and composition of carbonate associations from contrasting ore-related hydrothermal environments, the corresponding volcanic host rocks, and zones of weak alteration in Cabo de Gata Volcanic Belt in southeastern Spain and the Costal Range of central Chile. These new geochemical data suggest that hydrothermal carbonates related to ore formation can be clearly distinguished from sedimentary marine, metamorphic, and low-temperature carbonates. Furthermore, routine EPMA (Electron Probe Micro Analyser) chemical analysis of carbonates in ores could help to interpret their geochemical and isotopic composition by confirming the carbonates under investigation are directly related to ore-forming hydrothermal fluids.

2. Samples and Analytical Techniques

Samples for this study were collected from within volcanic and volcano-sedimentary terrains of Cretaceous-Cenozoic age (Table 1, Figure 1). In the Cabo de Gata Volcanic belt (southeast Spain), the Au-Cu Palai-Islica deposit was investigated. In the La Serena -29°3′–30°0′S- and Melipilla -33°50′ S- regions of Chile, several types of deposits were investigated, including: volcanic-hosted Au-Cu epithermal at El Dorado in La Serena; "Chilean Manto-type" Cu(-Ag), at Quebrada Marquesa in La Serena and Melipilla; stratabound Mn-rich hydrothermal deposit, at Quebrada Marquesa in La Serena; and Ag-Ba epithermal veins at Talcuna in La Serena.

Table 1. Summary of the main characteristics of the mineral deposits that hosts the studied samples.

	Palai-Islica (Spain)	**El Dorado (Chile)**	**Quebrada Marquesa (Chile)**	**Quebrada Marquesa (Chile)**	**Arqueros (Chile)**	**Melipilla (Chile)**
Deposit type	Epithermal Au-Cu volcanic-hosted	Epithermal Au-Cu volcanic-hosted	"Chilean Manto-type" Cu(-Ag)	Stratabound Mn	Ag-Ba epithermal veins	"Chilean Manto-type" Cu(-Ag)
Tectonic Setting	Extension after Alpine orogenesis	Compresional, arc setting	Extension, intra-arc basin	Extension, intra-arc basin	Extension, intra-arc basin	Extension, intra-arc basin
Morphology	Stockwork veins (and replacement)	Stockwork veins	Veins and replacement (stratabound)	Stratiform	Veins	Veins and replacement (stratabound)
Host rock	Andesites, dacites (*Carboneras C-3* Formation)	Andesites (*Los Elquinos* Formation)	Andesites, basaltic andesites (*Quebrada Marquesa* Formation)	Andesites, basaltic andesites (*Arqueros* Formation and *Quebrada Marquesa* Formation)	Andesites, basaltic andesites (*Arqueros* Formation)	Andesites, basaltic andesites, limestones (*Lo Prado* and *Veta Negra* Formations)
Hydrothermal alteration	Pervasive (argillic to propylitic)	Pervasive (argillic to propylitic?)	Not well developed. Associated with very low-grade assemblages?	Not well developed. Associated with very low-grade assemblages	Not well developed. Associated/oblite-rated? by very low-grade assemblages	Not well developed. Associated with very low-grade assemblages
Ore Mineralogy	Pyrite, chalcopyrite ± sphalerite, galena (gold, Ag-bearing minerals)	Pyrite, chalcopyrite ± fahlore (gold)	Chalcopyrite, bornite ± sphalerite, galena, chalcocite (fahlore, stromeyerite)	Braunite, piemontite (pyrolusite)	Ag, Ag sulfide, fahlore, bornite, chalcocite	Chalcopyrite, bornite, pyrite ± chalcocite (fahlore, arsenopyrite...)
Gangue Mineralogy	Quartz, sericite, chlorite, kaolinite, pyrophyllite (dolomite(-ankerite), barite, siderite)	Quartz, sericite, kaolinite (ankerite)	Calcite, barite (celadonite)	Calcite, barite	Calcite, barite (chlorite)	Calcite, celadonite, quartz, chalcedony
Age	Tortonian	Upper Creteceous - Paleocene?	Albian-Cenomanian	Lower Cretaceous	Albian-Cenomanian?	Albian-Cenomanian
Location	~1°55′ W Long., ~37°00′ N Lat.	~70°44′ W Long., ~29°47′S Lat.	~70°52′ W Long., ~29°54′ S Lat.	~70°54′ W Long., ~29°54′ S Lat.	~70°54′ W Long., ~29°51′ S Lat.	~71°01′ W Long., ~33°49′ S Lat.
References	[23–28]	[29]	[25,30–33]	[25,30–32]	[25,30–32]	[33]

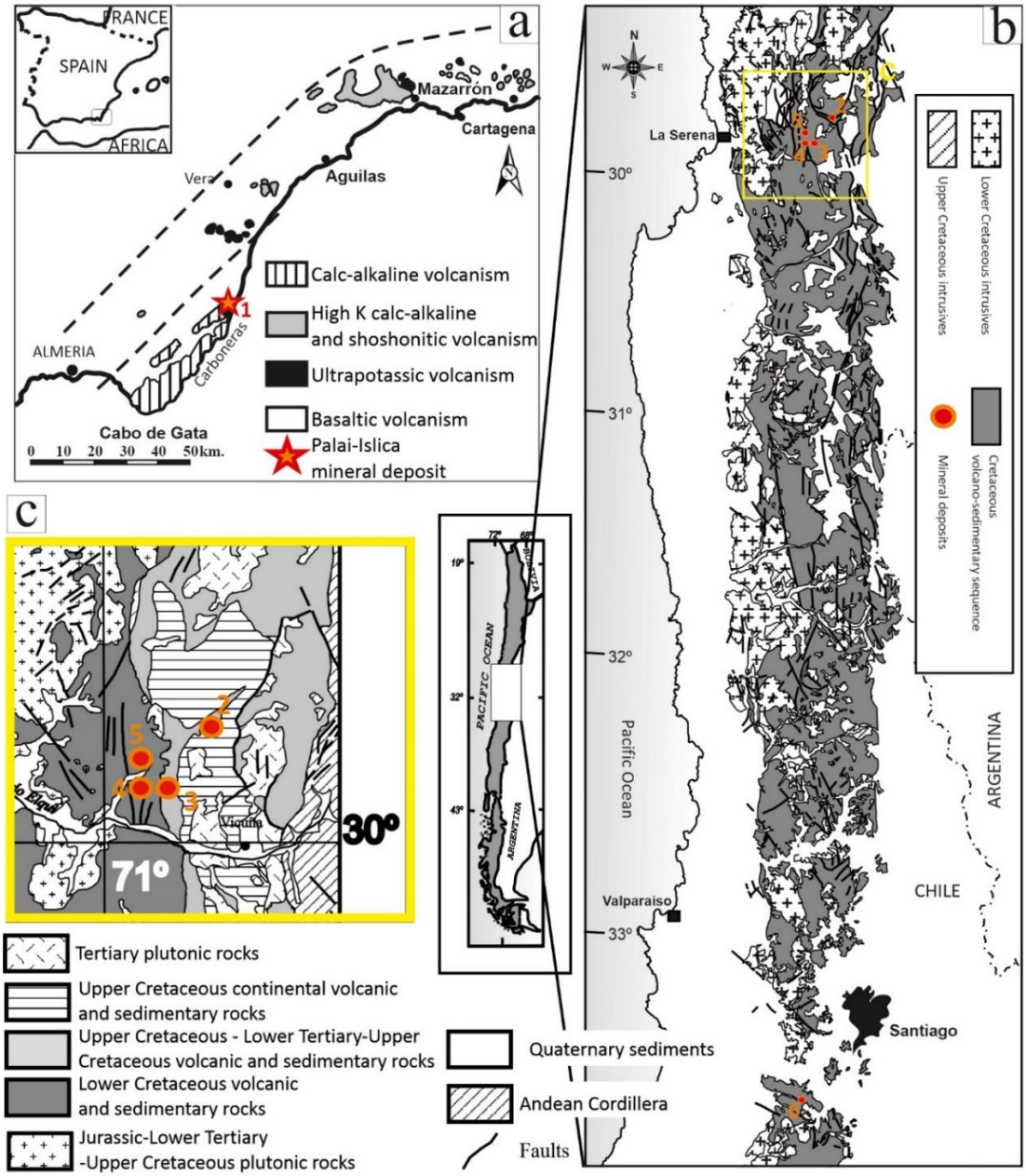

Figure 1. Geological framework of the studied areas. (**a**) Simplified geological map of the Cabo de Gata–Cartagena volcanic province in SE of Spain, with (1) the Palai-Islica, epithermal Au-Cu volcanic-hosted deposit, location (adapted from [23]). (**b**) Simplified geological map of the Lower Cretaceous belt in the Coastal Range of north-central and central Chile showing the studied deposits: (2) El Dorado-epithermal Au-Cu volcanic-hosted-, (3) Quebrada Marquesa—"Chilean Manto-type" Cu(-Ag)-, (4) Quebrada Marquesa-Stratabound Mn-, (5) Arqueros-Ag-Ba epithermal veins-, (6) Melipilla–"Chilean Manto-type" Cu(-Ag)-. (**c**) Geological map of La Serena area, where the majority of the studied deposits are located (adapted from [29,33]).

In addition to mineralized samples, carbonate samples were also collected from unmineralized host rocks close to each deposit in SE Spain and Chile affected by regional low-temperature hydrothermal alteration, and very low-grade metamorphism.

Petrographic observations were done using a transmitted and reflected light microscope and scanning electron microscopy (SEM) (ZEISS DSM 950). The geochemical composition of the studied minerals was characterized using an electron microprobe analyzer (EPMA) (CAMECA SX-50) of the "Centro de Instrumentación Científica" from the University of Granada. EPMA and SEM back-scattered images were used to determine the chemical composition and zonation of selected carbonates. A total of 559 micro-analyses

of carbonate were made with EPMA. The operating conditions were 20 kV accelerating potential, 20 nA beam current, 60 s X-ray peak and background acquisition times, and a specify wide beam in order to avoid damage to the crystal during analysis. Natural and artificial standards were used to calibrate quantitative analyses. The detection limit of different elements was around 0.05 wt. %.

3. Geological Setting and Mineralogical Features

3.1. Palai-Islica, Southeastern Spain

Palai-Islica is an intermediate and high sulphidation Au-Cu epithermal deposit hosted by hydrothermally altered Miocene calc-alkaline andesitic to dacitic rocks of the Cabo de Gata-Cartagena volcanic belt [23,28] (Table 1, Figure 1). This belt formed during extension of a thickened lithosphere during the Betic Orogeny (e.g., [34]). The mineralization consists of quartz veins with sulfides, some cases forming stockwork structures, and as replacement ore in zones of intense silicification. Details of the ore mineralogy and geochemistry of the deposit can be found in [23,24,26,27,35]. Quartz and white mica are the main gangue phases. Dolomite/ankerite and siderite, which are also common minerals, appear later in the paragenetic sequence, as micro-veinlets (Figure 2a), breccia cements of coarse equigranular grains, and sometimes rhombohedral crystals in the mineralized veins. Disseminated granular dolomite is also present in the hydrothermally altered volcanic host rocks, mostly replacing hornblende, pyroxenes, and plagioclase phenocrysts (Figure 2b). In addition, there is a regional replacement of mafic and plagioclase phenocrysts in volcanic rocks of the Cabo de Gata-Cartagena volcanic belt by calcite. Locally, unmineralized dolomite+calcite veins crosscut the volcanic rocks, and contain clasts of unaltered volcanic phenocrysts (Figure 2c). Toward the margin of the deposit, in the zone of propylitic alteration zone, dolomite is observed, replacing calcite (Figure 2d).

3.2. El Dorado, La Serena, Central Chile

El Dorado is an intermediate sulfidation Au-Cu epithermal deposit hosted by andesitic rocks of the Coastal Range of central Chile [29] (Table 1, Figure 1). It is located within the Upper Cretaceous *Los Elquinos* Formation (continental volcanoclastic dacites and andesites), associated with a zone of intense hydrothermal alteration. The available data for this Au-Cu prospect suggest that the style of mineralization is similar to the Palai-Islica deposit [25]. Ankerite is the predominant carbonate mineral found at El Dorado; ankerite in veins is subordinate to quartz and is paragenetically later than quartz and the main group of sulfides.

3.3. Quebrada Marquesa and Arqueros, La Serena, Central Chile

"Chilean Manto-type" Cu(-Ag), stratiform Mn, and Ag-Ba vein deposits coexist in the Coastal Range in the La Serena region within volcano and volcano-sedimentary sequences of Lower Cretaceous age [30,36,37] (Table 1, Figure 1). The *Arqueros* Formation (an Hauterivian-Barremian sequence of porhyric andesites and marine limestones) hosts Ag-Ba vein deposits, whereas the *Quebrada Marquesa* Formation (an Upper Barremian-Albian volcano-sedimentary sequence of andesites and continental sedimentary rocks, with minor intercalations of marine limestones and evaporites) hosts "Chilean Manto-type" Cu(-Ag) deposits. In addition, there are stratiform Mn deposits (oxides and silicate type) in the upper parts of the *Arqueros* Formation and mainly in the lower part of the *Qubrada Marquesa* Formation. Although the ore mineralogy of these deposits shows differences among them, they all share a gangue mineralogy dominated by calcite and barite [25,33] (Figure 2e). The host volcanic rocks range in composition from high-K calc-alkaline basaltic andesites to andesites [38], which underwent extensive very low-grade metamorphism [39], with amygdules commonly filled by prehnite and coarse calcite (Figure 2f).

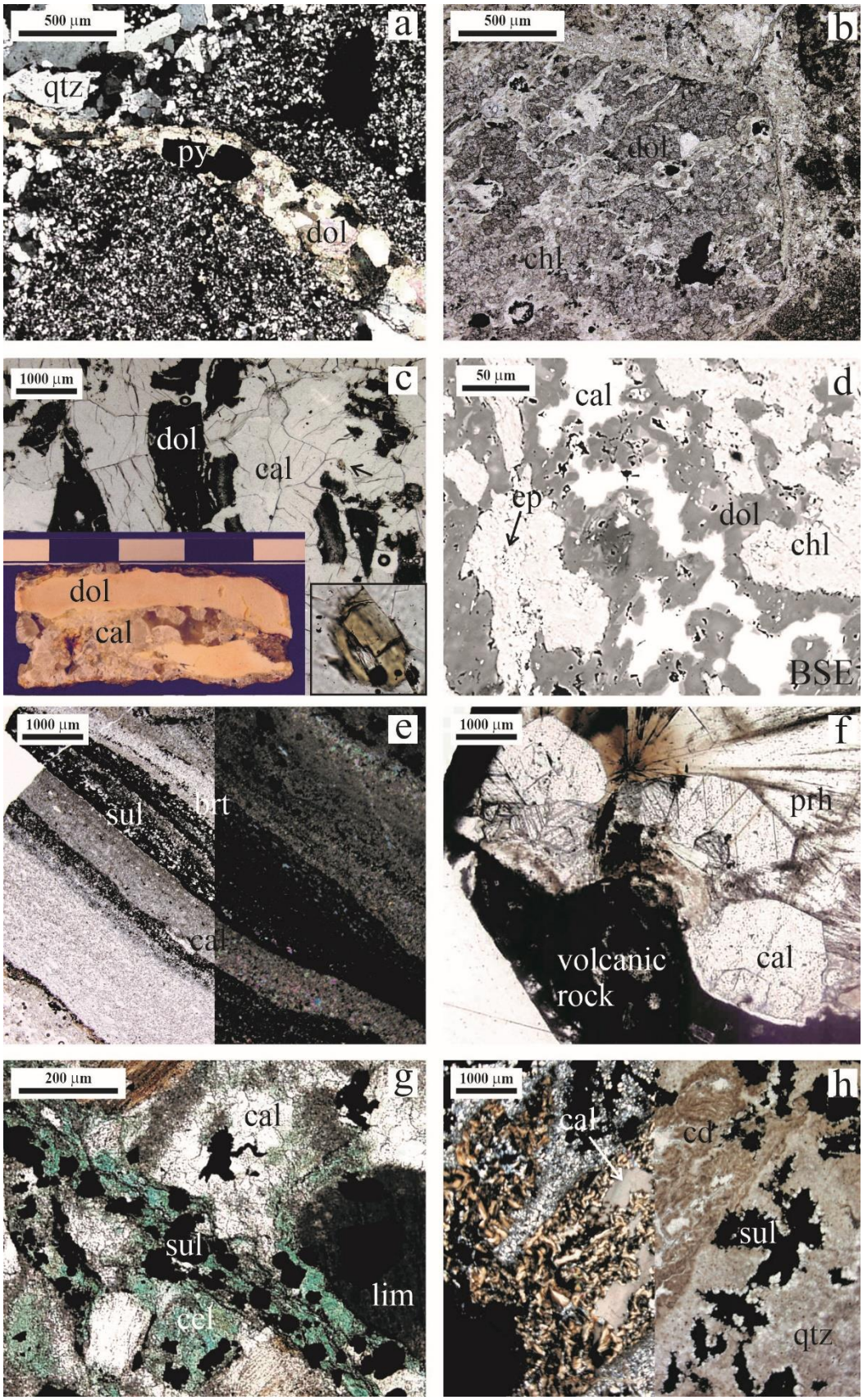

Figure 2. Transmitted light photomicrographs, back-scattered electron (BSE) images, and hand specimen photographs of different carbonates associated with hydrothermal ore deposits and associated host rocks. (**a**) Ore-related dolomite/ankerite (dol) microvein with pyrite (py) crosscutting an earlier quartz vein, in the Au-Cu epithermal Palai-Islica (SE Spain) deposit. (**b**) Dolomite/ankerite

(dol) and chlorite (chl) replacing volcanic hornblende in pervasive hydrothermal alteration of andesites and dacites in Palai-Islica. (**c**) Unmineralized dolomite (dol) + calcite (cal) veins crosscutting the volcanic rocks of the Cabo de Gata volcanic belt with unaltered hornblende clasts (indicated by an arrow). (**d**) Dolomite (dol), associated with epidote (ep) and chlorite (chl), replacing calcite (cal) in distal, propylitic-type, hydrothermal alteration of the Palai-Islica deposit. (**e**) Banded vein of sulfides (sul) with calcite (cal) and barite (brt) in the Quebrada Marquesa (La Serena, central Chile) "Chilean Manto-type" Cu(-Ag) deposit. (**f**) Amygdule infilling of calcite (cal) and prehnite (prh) related to very low-grade metamorphism in an andesite from the La Serena area. (**g**) Polymetallic-ore association at Melipilla "Chilean Manto-type" Cu(-Ag) mineralization, with calcite (cal) and celadonite (cel) associated with sulfides and with clasts of host limestone (lim). (**h**) Late calcite (cal) filling associated with low-grade disseminated sulfide (sul) ore.

3.4. Melipilla, Central Chile

"Chilean Manto-type" Cu(-Ag) mineralization in Melipilla occurs in limestones, mudstones and andesites of the *Lo Prado* (Berrian-Hauterivian) and *Veta Negra* formations (Hauterivian-Barremian), part of the Coastal Range [33]. Two ore types exist: a low-grade, bornite-chalcocite disseminated mineral association and a sulfide-rich polymetallic mineral association [33]. Both styles of mineralization contain calcite as a gangue phase. However, in the low-grade disseminated mineralization, it appears as void infilling (late phase), subordinate to quartz, whereas in the sulfide-rich polymetallic association, it is the main gangue phase (Figure 2g,h). Clasts of limestone host rocks within the mineralization are observed in addition to calcite gangue (Figure 2g). The andesitic host rocks were subject to very low-grade metamorphism, with calcite a common mineral of this regional alteration in the form of microveins and amygdule infill.

4. Elemental Composition of Carbonate Minerals

4.1. Epithermal Au-Cu Volcanic-Hosted Deposits, Palai-Islica and El Dorado

The results of the EPMA analyses of dolomite/ankerite for the Palai-Islica and El Dorado deposits are summarized in Table S1 and plotted in Figures 3–5. In the Palai-Islica deposits, there is a large range of Ca (5.43–11.05 at. %), Mg (5.69–10.16 at. %), Fe (0.03–4.41 at. %), and Mn (0.18–2.27 at. %), with clear chemical differences between different generations of dolomite/ankerite. For example, dolomite/ankerite in the orebody has the widest range of Fe and Mn values, with a heterogeneous spatial distribution and a long tail to higher Fe and Mn contents toward the ankerite field. Dolomite from barren veins in volcanic rocks shows the lowest Fe and Mn contents (below 0.25 at. %), and is quite homogeneous (Figure 4). Dolomite in the hydrothermal alteration shows a considerable compositional range (up to 1.75 at. % Fe and 1.04 at. % Mn, Figure 4). Nevertheless, the modes for the Fe and Mn contents obtained for dolomite within the hydrothermal alteration coincide with the modes for Fe and Mn obtained from dolomite in the orebody (Figure 4). The Fe and Mn contents are approximately proportional at 2:1 (Figure 5a), with the majority of the analysis showing an inverse correlation between Fe+Mn and Mg, with the exception of carbonates, showing the highest Fe+Mn contents (Figure 5b).

Siderite crystal occurs as an accessory phase in the orebody. It shows a variable composition (Table S1, Figure 3). The major elements, Mg (0.19–3.58 at. %), Mn (1.11–3.55 at. %), and Ca (0.10–2.54 at. %), are approximately proportional to the Fe content, which ranges between 9.46 and 16.83 at. %.

The calcite composition (Table S1, Figure 3) reveals concentrations of Fe (0–0.75 at. %), Mg (0.01–0.52 at. %), and Mn (0.00–0.30 at. %), which differ among sample sites. Calcite from regions of propylitic hydrothermal alteration shows significantly higher Mn contents (0.07–0.30 at. %) than for regional alteration and barren veins (<0.05 at. %). The calcite from these systems also shows a relatively high abundance of Fe and Mg, with a correlation between the Mg and the Mn and Fe contents (Figure 5c,d).

Back-scattered SEM images of Palai-Islica carbonates reveal chemical zonation in dolomite/ankerite crystals from the orebody (Figure 6), which typically depict a concentric

pattern, in some cases oscillatory, with a dark core and a bright rim. This pattern reflects a rim depleted in Mg and enriched in Fe and, in some cases, Mn. The composition of a single crystal can almost record the entire chemical variation observed for a given population (Figures 4 and 6).

Ankerite from the El Dorado orebody has a composition (Table S1, Figure 3) with similarities to dolomite/ankerite of Palai-Islica. The range of Ca (7.57–11.06 at. %), Fe (2.36–5.29 at. %), and Mn (0.32–1.02 at. %) overlaps the range of data from the Palai-Islica carbonates. Although carbonates with a similar Fe content from El Dorado show an increased Ca content and less Mn than observed in the Palai-Islica samples, no proportional relationship between Fe and Mn is observed in El Dorado ankerites. In addition, the Mg content (3.45–6.47 at. %) of ankerite from El Dorado is consistently lower than in Palai-Islica ankerite.

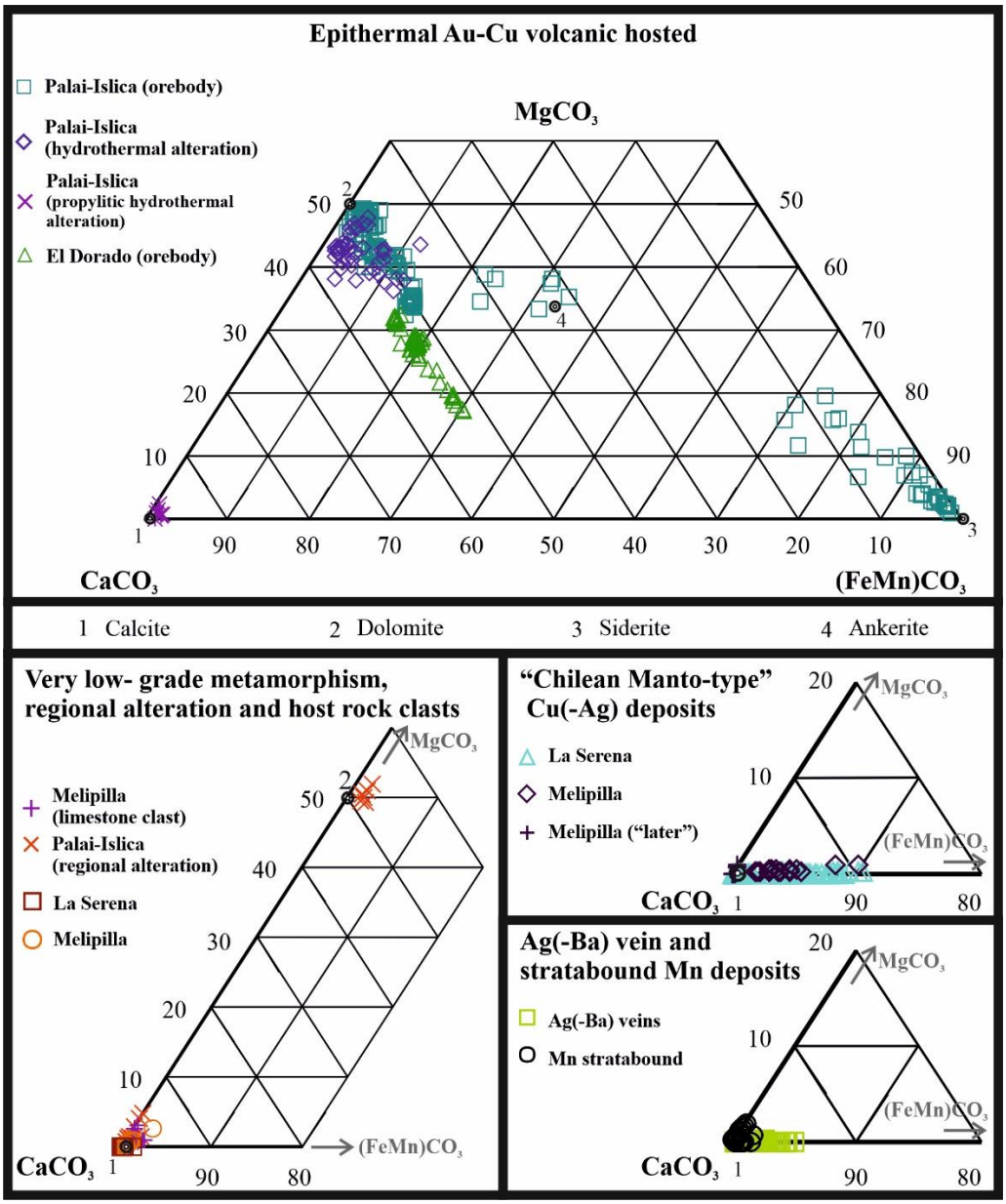

Figure 3. Triangular plot ($CaCO_3$-$MgCO_3$-$FeCO_3$+$MnCO_3$) showing the major molar composition of analyzed carbonates. According to the carbonate type in each location, only a portion of the triangles is shown.

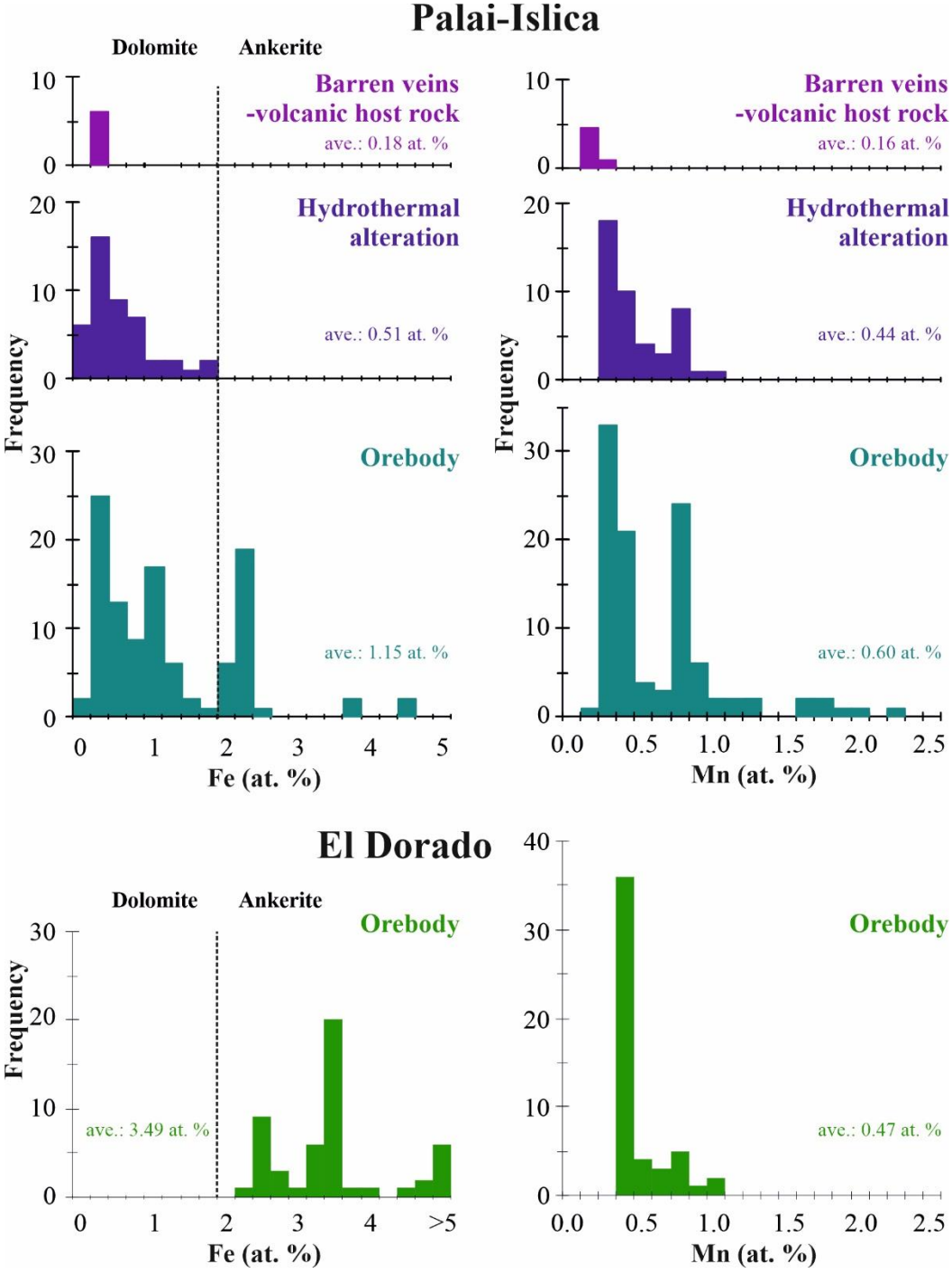

Figure 4. Frequency histograms for the Fe and Mn content in atomic % for the dolomite/ankerite analyzed from the Au-Cu epithermal deposit (Palai-Islica-SE Spain, and El Dorado-central Chile).

Back-scattered SEM images of ankerite at El Dorado reveal irregular and oscillatory chemical zonation (Figure 7). The oscillatory rims have a relatively low Fe content, whereas irregularly zoned cores have a significantly higher Fe and Mn content.

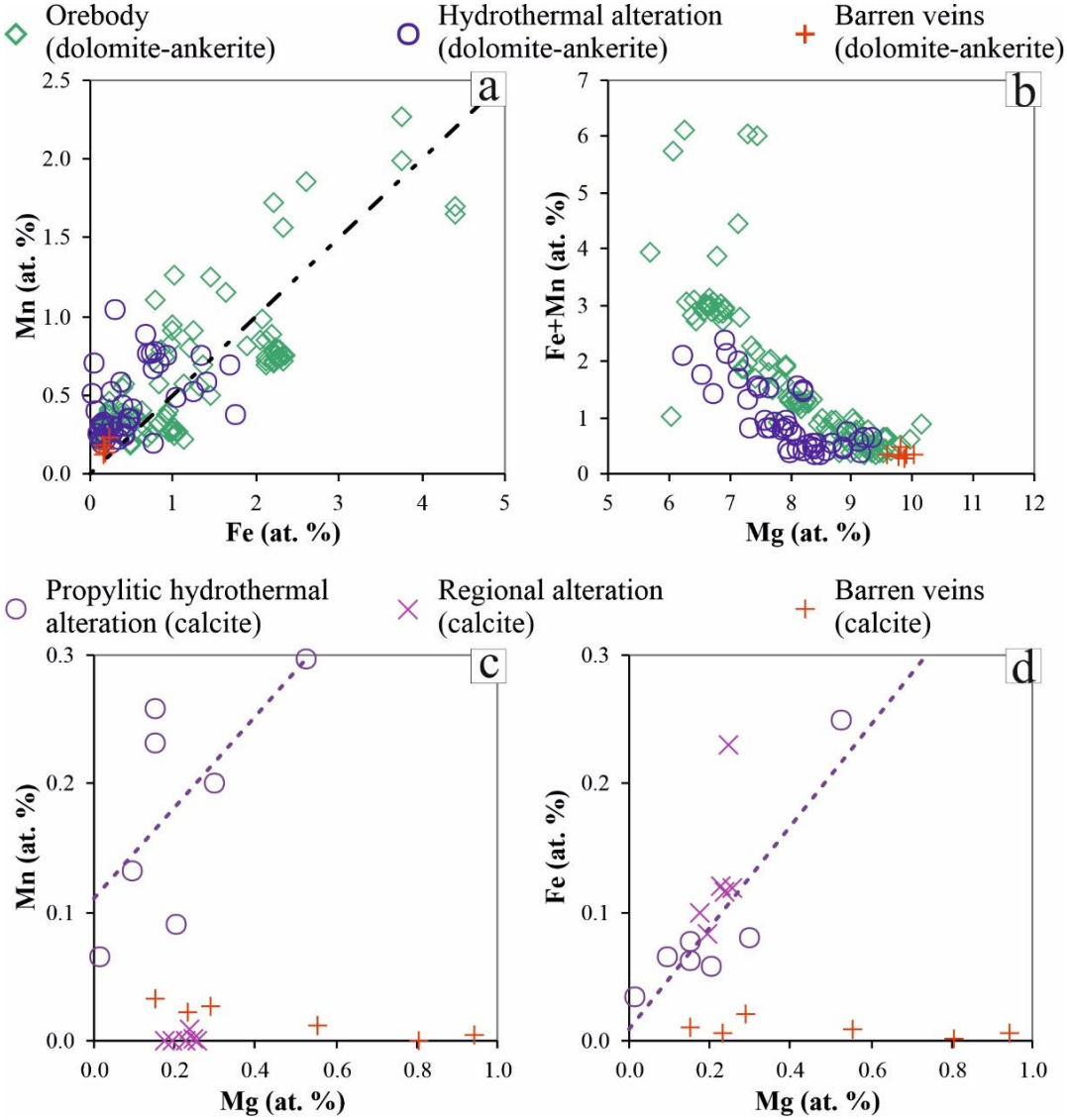

Figure 5. Composition of carbonates from Palai-Islica area (SE Spain): (**a**) Fe vs. Mn and (**b**) Mg vs. Fe+Mn in dolomite/ankerite: orebody, hydrothermal alteration, and barren veins in the volcanic rocks of the Cabo de Gata-Cartagena volcanic belt belonging to a regional alteration. The dotted line marks in (**a**) a Fe:Mn relation of 2:1. (**c**) Mg *vs.* Mn and (**d**) Mg *vs.* Fe in calcite: propylitic hydrothermal alteration, regional alteration in the volcanic rocks of the Cabo de Gata volcanic belt, and barren veins in the volcanic rocks of the Cabo de Gata volcanic belt. The dotted colored lines mark, respectively, in (**c**) and (**d**) the correlation between Mg and Mn ($r^2 = 0.46$) and Mg and Fe ($r^2 = 0.85$) in calcite from the propylitic hydrothermal alteration.

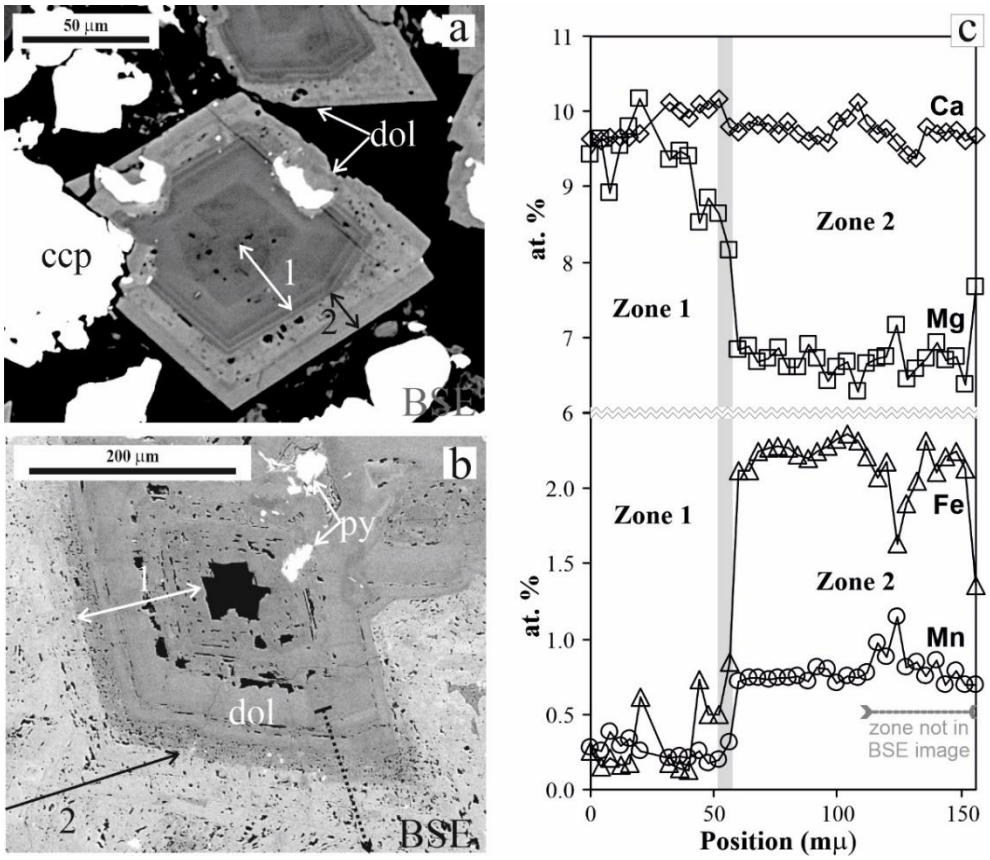

Figure 6. Back-scattered electron (BSE) images (**a**, **b**) of zoned dolomite/ankerite from the Palai-Islica orebody (SE Spain) in which two main zones 1 (earlier and darker in BSE), and 2 (later and brighter in BSE) are distinguished. In (**c**), a profile through the crystal of picture b (indicated by a dotted line, which end is out of the picture) is shown, being represented Mg, Ca, Fe, and Mn atomic % contents.

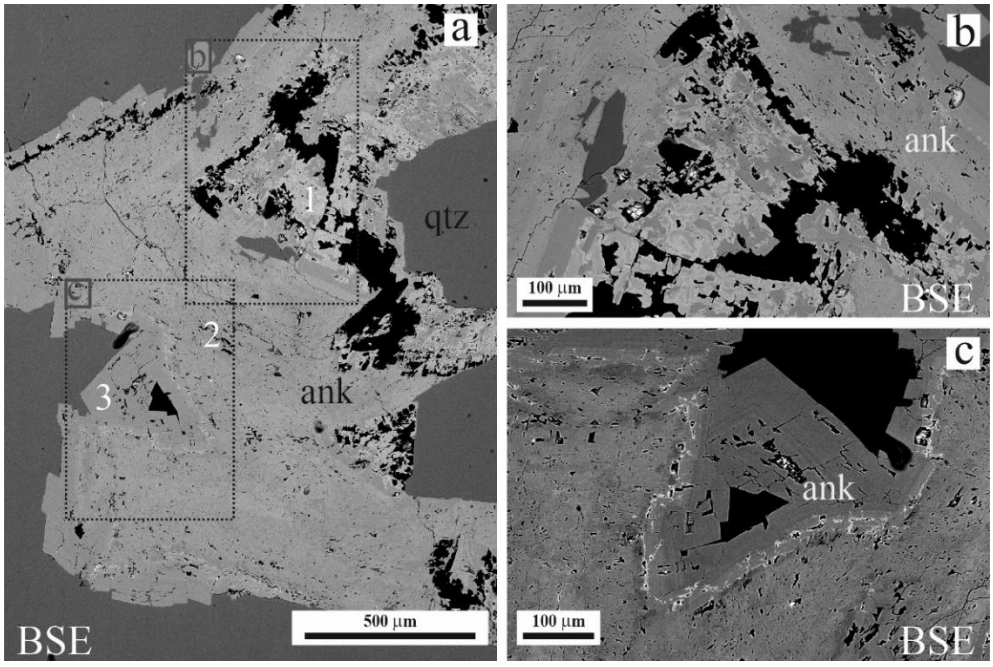

Figure 7. Back-scattered electron (BSE) images of zoned ankerite aggregate crystals in the El Dorado Au-Cu orebody (central Chile). Three zones are observed: (1) highly irregular zoned cores, with the highest Fe and Mn content; (2) porous weak zoned zone and overgrowth; with (3) weak oscillatory zonations and the lowest Fe and Mn content. Images (**b**,**c**) show details of the rectangle areas of image (**a**).

4.2. "Chilean Manto-Type" Cu(-Ag) Deposits, Quebrada Marquesa in La Serena and Melipilla

The composition of calcite, a major gangue phase in these deposits, is compiled in Table S2 and Figures 3 and 8. Calcite from the Quebrada Marquesa, La Serena, and Melipilla polymetallic deposits shows relatively high Mn contents (0.01–1.92 at. %; average 0.57 at. %), and low Fe contents (0.00–0.45 at. %; average 0.09 at. %). The amounts of Fe and Mn correlate poorly (Figure 8a), but with a higher slope to the data from the Melipilla polymetallic association, compared to the Quebrada Marquesa data. The Melipilla data also show lower Fe contents than the polymetallic association at Quebrada Marquesa (Figure 8a). The level of Mg in calcite from both localities broadly correlates with Mn+Fe (Figure 8b), although calcite from the Melipilla polymetallic association is richer in Mg than in Quebrada Marquesa (0.03–0.18 at. % and 0.00–0.05 at. %, respectively). It is noteworthy that the lowest Mn and Fe contents were recorded in late calcite from the Melipilla low-grade disseminated mineral association, but with a slightly elevated Mg content of 0.00- 0.16 at. % (Figure 8a,b). Finally, calcite from limestone host rock clasts within the mineralization are also Mn and Fe poor (Mn: 0.01–0.28 at. %; Fe: 0.01–0.11 at. %) but with a relatively high Mg content (0.06–0.63 at. %).

Calcite from these "Chilean Manto-type" Cu(-Ag) deposits is also commonly zoned, as shown by the back-scattered SEM images. The zonation is complex, commonly with a morphology resembling "caries" textures or forming a patchwork (Figure 9). Back-scattered images show that paragenetically late calcite is commonly dark and Mn- and Fe-poor, compared to the initial or earlier calcite, which itself has a variable Mn-Fe content.

4.3. Other Deposits: Ag-Ba Vein and Stratabound Mn Deposits (Quebrada Marquesa and Arqueros in La Serena)

Calcite compositions (Table S3) from a stratabound Mn deposit in Quebrada Marquesa are characterized by low Mn and Fe contents (Mn: 0.00–0.32 at. %; Fe: 0.00–0.02 at. %, Figure 8c,d) and high Mg contents (0.00–0.36 at. %). In contrast, calcite from the Ag-Ba veins in Arqueros has relatively high Mn and Fe (Mn: 0.03–0.94 at. %; Fe: 0.00–0.12 at. %) with a low Mg content (0.00–0.03 at. %, Figure 8c,d). Notably, calcite from veins richer in total metal content (mainly Cu, although poorer in Ag) have appreciable higher Fe and Mn contents (Mn: 0.05–0.94 at. %; Fe: 0.00–0.12 at. %, Figure 8c,d) compared to calcite from veins with lower total metal contents (Mn: 0.03–0.27 at. %; Fe: 0.00–0.02 at. %, Figure 8c,d). Back-scattered SEM images of calcite from the Ag-Ba veins resemble carbonate crystals from the "Chilean Manto-type" Cu(-Ag) deposits, with similar "caries"-like textures (Figure 10). Truncations of oscillatory banded calcite are also observed. In the case of the Mn deposits, bright cores (Mn-Fe rich) are embedded in dark calcite with a tendency toward a lower Mn(-Fe) content as precipitation progresses.

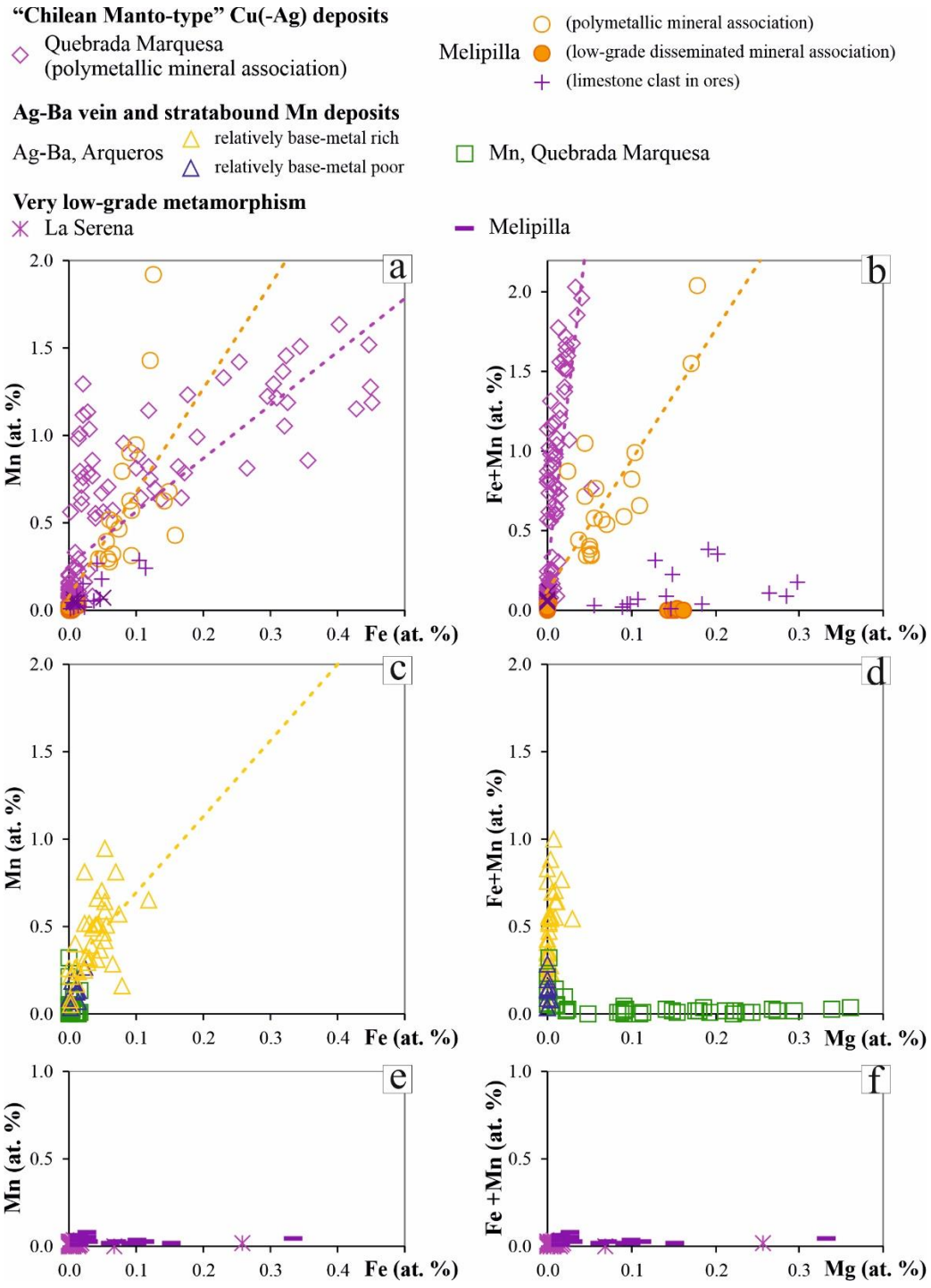

Figure 8. Fe vs. Mn and Mg vs. Fe+Mn in atomic % showing the composition of calcite from different mineralizations/very low-grade metamorphism in central Chile: (**a**,**b**) "Chilean Manto-type" Cu(-Ag) deposits (Quebrada Marquesa -La Serena- and Melipilla, central Chile): Quebrada Marquesa polymetallic mineral association; Melipilla polymetallic mineral association; late calcites from Melipilla low-grade disseminated mineral association; calcite from limestone host rock in Melipilla polymetallic association. The dotted colored lines mark in (**a**) the correlation line between Fe and Mn (r^2= 0.62 for Quebrada Marquesa and r^2= 0.22 for Melipilla polymetallic association) and Mg and Fe+Mn (r^2= 0.58 for Quebrada Marquesa and r^2= 0.62 for Melipilla polymetallic association) in the propylitic hydrothermal alteration calcites. (**c**,**d**) Stratabound Mn deposits (La Serena, central Chile) and Ag-Ba veins (relatively base-metal rich and relatively base-metal poor). The dotted colred line marks in (**a**) the correlation line between Fe and Mn (r^2= 0.27) in calcite from Ag-Ba, relatively base-metal rich, veins. (**e**,**f**) Very low-grade metamorphism in volcanic rocks from La Serena and Melipilla areas (central Chile).

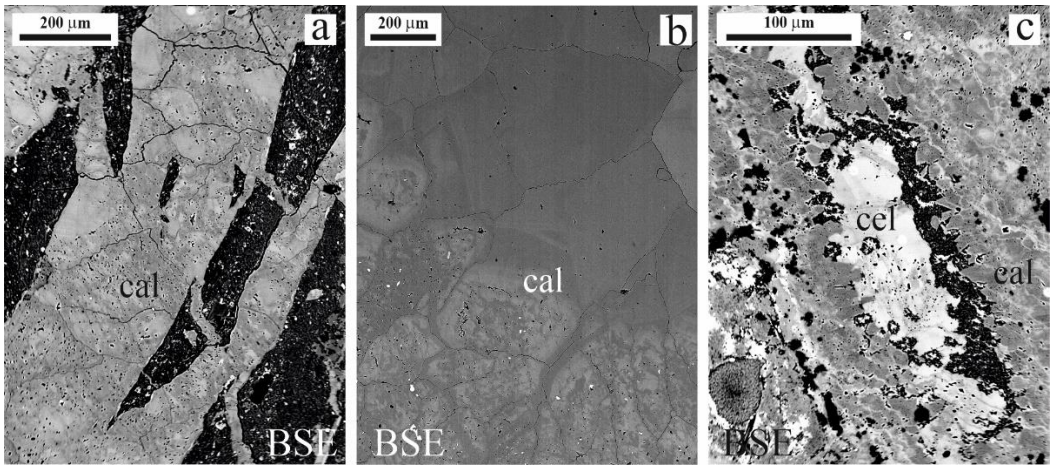

Figure 9. Back-scattered electron (BSE) images of zoned calcite aggregates crystals from "Chilean Manto-type" Cu(-Ag) deposits: (**a**,**b**) Quebrada Marquesa-La Serena- and (**c**) Melipilla (central Chile).

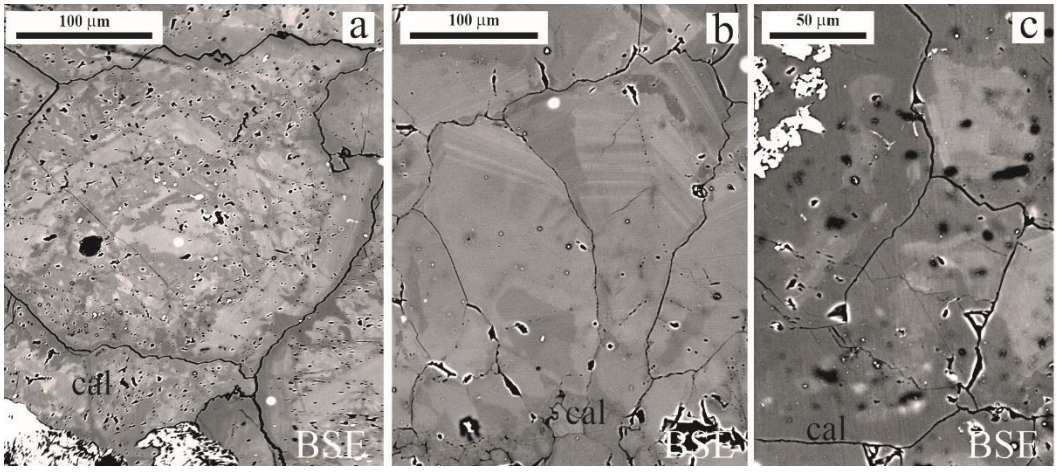

Figure 10. Back-scattered electron (BSE) images of zoned calcite aggregates crystals from: (**a**,**b**) Ag-Ba veins and (**c**) stratabound Mn deposits (La Serena, central Chile).

4.4. Very Low-Grade Metamorphism (La Serena and Melipilla)

Calcite filling vacuoles, in veins, or as replacement of phenocrysts associated with low-grade metamorphic assemblages in the volcanic rocks show compositions (Table S4) characterized by very low Mn contents (0.00–0.08 at. %, Figure 8e,f) both in La Serena and Melipilla. The Mg content is generally very low at La Serena (0.00–0.01 at. %) but relatively high (0.00–0.46 at. %) at Melipilla (Figure 8f).

5. Discussion

Fluid inclusion, field-based [23,27,28], and petrographic observations from the Palai-Islica deposit show that dolomite/ankerite originated through hydrothermal activity, both in the orebody and the associated zones of hydrothermal alteration. Siderite, although less common, shares the same origin but is restricted to the shallow parts of the deposit. It probably crystallized at lower pH due to a magmatic SO_2 input into the ore fluids producing disproportionation [27,28], mixed with oxidizing surface fluids (seawater and meteoric waters in an indeterminate proportion).

In contrast, the calcite observed originated by a non-mineralization-related hydrothermal process, involving circulation of seawater and eventually later meteoric phreatic waters along fractures, producing barren calcite-dolomite veins and calcite replacement of magmatic phenocrysts of the volcanic rocks. This is a regional process, which probably

was triggered by the tectonic activity associated with the Carboneras strike-slip fault [40], where evidence of low-temperature fluid flow has been documented [41]. This fluid migration began, at least in the Palai-Islica area, before mineralization (~10–9 Ma, [28]), and just after the formation of volcanic host rocks to the Au-Cu mineralization (10.4 Ma, [42]).

The formation of either dolomite or calcite, in addition to fluid chemistry, is most likely related to the precipitation temperature, as higher-temperature fluids tend to precipitate dolomite, whereas lower-temperature fluids typically form calcite [43] (Figure 11). The Mg content could be derived from the leaching of volcanic rocks. Therefore, the carbonate mineralogy in this volcanic environment reflects the contrasting environments of deposition with the presence of dolomite (± siderite) related to the presence of mineralized orebodies.

The mineral composition of the carbonates in the Palai-Islica deposit, with dolomite/ankerite generally Mn- and Fe-rich (Figure 4), offers insights into the mineralization processes. Dolomite/ankerite from the orebody tends to be more heterogeneous in composition, with higher contents of Mn and Fe than dolomite from the associated zones of hydrothermal alteration. Both Mn and Fe show subtle variations and also a significant increase in the outer zone of dolomite/ankerite crystals (zone 2 in Figure 6). This probably reflects the chemical complexity of the hydrothermal fluids [23,24,26–28], and an increase in the Mn and Fe content of the hydrothermal fluids may be associated with a recharge of deep hydrothermal metal-bearing fluids, which is coherent with the geochemical and isotopic evidence [23,28].

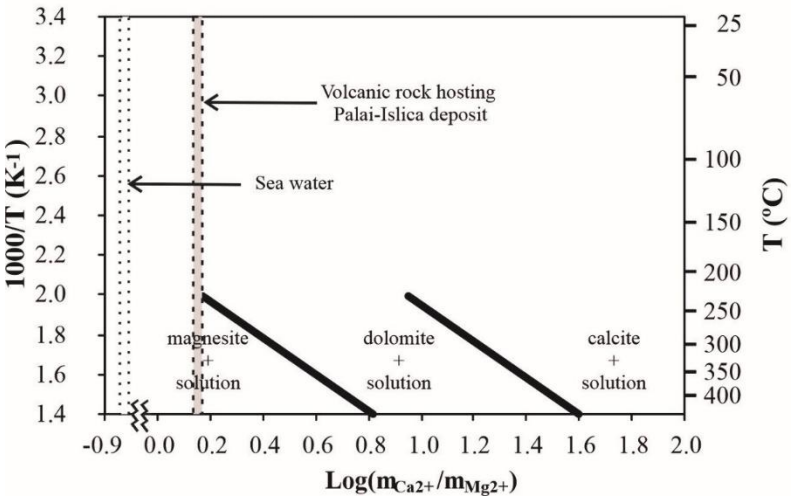

Figure 11. Binary diagram showing the stability fields of calcite, dolomite, and magnesite as the Ca/Mg activity ratio and temperature function. The stability limits were calculated from replacing conditions of one phase by others (adapted from [43]). For reference, marine water [44] and the Ca/Mg ratio of unaltered andesites/dacites hosting Palai-Islica deposit [45] are also shown.

The elevated but more restricted Mn content of the hydrothermal alteration may reflect the buffering capacity of the host volcanic rocks (typically 0.12 MnO wt % [45]). In contrast, dolomite from barren veins shows lower Mn and Fe contents, which confirms the notion that elevated Mn and Fe concentrations correlated with the mineralizing process. As it is suggested above, these barren veins could originat from the circulation of surface waters.

The composition of calcite also correlates with the geological setting and mineral paragenesis. Calcite replacing phenocrysts, and in barren veins, and dolomite within the volcanic rocks of the Cabo de Gata volcanic belt are both Mn-poor; however, calcite from the propylitic alteration around the Palai-Islica deposit is relatively Mn-rich (and also Fe-rich). In addition, Fe is relatively higher in calcite replacing volcanic phenocrysts, suggesting that this is an inherited feature of the mafic phenocrysts with a high Fe content [40]. Local

redox processes [46], perhaps reflecting a reducing process of the surface waters by reaction with the andesite/dacite host rocks, could also be relevant. The Mg content of calcite from the barren veins is typically elevated, possibly due to a relatively higher temperature of formation of these veins according to the calcite-dolomite geothermometer when calcite and dolomite coexist [47]. Therefore, in the Palai-Islica area, the Mn (and in some cases, Fe) content of carbonates is an excellent indicator of a hydrothermal, and potentially ore-related, origin.

At the El Dorado epithermal Cu-Au deposit, ankerite is typically found within veins with sulfides. The ankerite is Mn- and Fe-rich, with Fe contents much higher than in ankerite from Palai-Islica. At El Dorado, the zonation of ankerite crystals (Figure 7) suggests that the chemical evolution of the carbonate, evidenced by contrasting chemical zones, is the opposite to that at Palai-Islica, with a slight decrease of the Mn and Fe content in ankerite crystals with time. This chemical evolution was perhaps due to the progressive input of oxidizing meteoric fluids, in the latest stage of the hydrothermal-magmatic system that produced the ore mineralization.

The presence or absence of dolomite/ankerite and calcite at the Palai-Islica or El Dorado deposits is linked to the style of mineralization. Both deposits are considered intermediate/(high)-sulfidation epithermal deposits [27–29], which, by definition, usually lack carbonates as a significant gangue phase. They contrast with low-sulfidation epithermal deposits, which commonly have calcite as a gangue phase (e.g., [48,49]). The timing of dolomite precipitation, late in the paragenetic evolution of the Palai-Islica and El Dorado intermediate(/high)-sulfidation epithermal deposits, is consistent with the pH of the ore fluids having been neutralized by their interaction with the host rocks and the acquisition of sufficient Mg to form dolomite rather than calcite.

The "Chilean Manto-type" Cu(-Ag), Ag-Ba veins, and stratabound Mn deposits investigated from central Chile have calcite ± barite as major gangue minerals and are hosted within volcanic rocks, typically of andesitic composition, and sedimentary rocks. The existence of calcite rather than dolomite suggests that the activity of Mg^{2+} in the ore-forming fluids was relatively low, because even at low Mg/Ca values at the typical range of epithermal temperatures (i.e., 150–250°C), dolomite should precipitate rather than calcite [43] (Figure 11).

In the polymetallic association of "Chilean Manto-type" Cu(-Ag) deposits, the calcite is Mn-rich and, to a lesser extent, Fe-rich (Figure 8a,b). Calcite in Ag-Ba veins is less Fe-rich and less Mn-rich than calcite from "Chilean Manto-type" Cu(-Ag) deposits (Figure 8), which also correlates with the lower sulfur and metal content of these veins. Consideration of the calcite data exclusively from Ag-Ba veins shows that veins with higher metal contents give higher Mn and Fe contents than calcite from Ag-Ba veins with lower total metal contents (Figure 8c,d). Finally, calcite from very low-grade metamorphic rocks hosting the stratabound deposits are always Mn-poor, and in the case of La Serena, also Fe and Mg-poor (Figure 8e,f). Therefore, these deposits invariably preserve the correlation between the Mn content of calcite and associated mineralization, which reflects the Mn content of the hydrothermal fluids, and metal content (mainly Cu) of hydrothermal fluids.

It is also noteworthy that carbonates in the stratabound Mn deposits are Mn (and Fe)-poor. The explanation for the low Mn content could be because the hydrothermal fluids that precipitated the low Mn calcite and barite were not related directly to Mn-ore precipitation but precipitated in a later stage, being dominated by oxidizing meteoric waters with a low Mn content. Petrographically, the calcite in this deposit is clearly associated with Mn ore minerals, although it is observed that calcite postdates Mn minerals in the mineral paragenesis. In either case, further fluid inclusion and isotopic studies performed in this calcite could decipher fluids related to late-stage ore formation or recrystallization of Mn-ores instead of the conditions extant during the formation of primary Mn ores. An equivalent argument could be made for calcite from Melipilla low-grade disseminated mineral association, also witha very low Mn (and Fe) content (Figure 8a,b) and paragenitically late.

These new data on the mineral compositions of carbonates clearly support the idea previously described that Mn can be used a as whole-rock element index of hydrothermal-ore bearing activity (e.g., [18,19]) and previous studies that showed elevated concentrations of Mn (and Fe) in carbonates related to precious and base-metal hydrothermal deposits (e.g., [6,15–17]). In contrast, where the carbonates are paragenetically late or unrelated to the mineralization, they show markedly lower Mn contents (0.00–0.08 at. %, in contrast with associated ore mineralization, with up to 1.63 at. %). This Mn depletion was also noted in the hydrothermal Irish Zn-Pb ore-field [6]. Moreover, these observations are consistent with measurements of the Mn content of different types of hydrothermal fluids (Table 2). Although there are several factors that control Mn incorporation into calcite (kinetics of precipitation; composition of the fluid, particularly the Mn/Ca ratio; precipitation of other minerals (e.g., [46,50,51])), simple calculations with distribution coefficients estimated for temperatures ranging between 150 and 250°C, constrained by fluid-inclusion data in the studied carbonates (references in Table 1), suggest the potential of ore-forming fluids to produce Mn-rich calcite (Table 2).

Furthermore, with the measured Mn calcite content, and assuming different Ca concentrations of the fluids (fluid-inclusion data suggest a relatively high Ca content in Chilean samples [32]), the Mn content of the hydrothermal and metamorphic fluids was estimated. These Mn values, according to the performed calculations, could be considerably higher than 100 μMol/kg for the "Chilean Manto-type" Cu(-Ag), and Ag-Ba veins, whereas for the very low-grade metamorphism and calcite from the Mn stratabound deposit it could be two orders of magnitude lower (Table 3).

Table 2. Range of concentrations of Mn and Ca found in different types of fluids.

	Mn (μMol/kg)	Ca (μMol/kg)	Mn at.% (Calcite)		
			150°C	200°C	250°C
Hydrothermal sea vents[1]	15	22000	0.11	0.07	0.04
	6800	80000	14.03	8.93	5.53
Geothermal fluids[2,3]	0	7	0.42	0.27	0.17
	146	699	25.00	21.89	13.55
Metamorphic fluids[2]	0	136	0.00	0.00	0.00
	5	475	1.74	1.10	0.68
Sea water[1]	0	10200	0.00	0.00	0.00

Note: Data from compilations of 1: [52]; 2: [53]; 3: [54]. Estimations of Mn concentration (in atomic %) in calcite precipitating from these fluids assuming distribution coefficients [46] at temperatures from 150 to 250°C, and the extreme Mn and Ca values for these different types of fluids.

Table 3. Estimates of the Mn content of hydrothermal/metamorphic fluids from the studied areas according to the concentration of Mn in calcites precipitated (minimum, maximum, and average Mn content), the distribution coefficient of [46], and different possible values of Ca in the hydrothermal fluids.

	Mn (at.%) calcite	Mn (μMol/kg) 150 °C			Mn (μMol/kg) 200 °C			Mn (uMol/kg) 250 °C		
		A	B	C	A	B	C	A	B	C
Quebrada Marquesa ("Manto-type" Cu(-Ag))	0.01	0	2	4	1	3	7	1	5	11
	1.63	101	504	1008	158	792	1584	256	1280	2559
	0.51	**31**	**156**	**313**	**49**	**246**	**491**	**79**	**397**	**793**
Melipilla ("Manto-type" Cu(-Ag))	0.28	17	86	172	27	136	271	44	219	438
	1.92	119	593	1186	186	932	1863	301	1505	3010
	0.65	**40**	**200**	**400**	**63**	**314**	**628**	**101**	**507**	**1015**
Quebrada Marquesa (Ag-Ba veins)	0.03	2	10	20	3	16	31	5	25	50
	0.94	58	291	583	92	458	916	148	740	1480
	0.37	**23**	**115**	**230**	**36**	**180**	**361**	**58**	**291**	**583**
Arqueros (stratabound Mn)	0.00	0	0	0	0	0	0	0	0	0

	0.32	20	100	200	31	157	315	51	254	508
	0.04	**3**	**13**	**26**	**4**	**21**	**42**	**7**	**34**	**67**
Very low-grade metamorphism	0.00	0	0	0	0	0	0	0	0	0
	0.08	5	26	52	8	41	82	13	66	132
	0.02	**1**	**6**	**11**	**2**	**9**	**17**	**3**	**14**	**28**

Note: Calculated with a concentration of Ca of equivalent x times sea water Ca content: (A) 1; (B) 5; (C) 10.

The chemical zonation in carbonate minerals from "Chilean Manto-type" Cu(-Ag), Ag-Ba veins, and stratabound Mn deposits is consistent with fluctuations in the chemistry of hydrothermal fluids (Figures 9,and 10). The textures in "Chilean Manto-type" Cu(-Ag), and Ag-Ba veins such as "caries" texture (Figures 9 and10) suggest dissolution reprecipitation of calcite, which reflects changes during hydrothermal activity. In both cases, similar textures are found, a fact that could indicate that in the La Serana area "Chilean Manto-type" Cu(-Ag), and Ag-Ba veins are deposits with a clear genetic link. Furthermore, in both cases, the late calcite is Mn and Fe poor. In other context, such in low low-temperature fluid systems developed in the Pyrenees during its tectonic evolution, calcite also shows a late Mn and Fe decrease. This chemical evolution has been interpreted as the system was dominated by low-temperature meteoric waters due to uplifting processes. In our case, this chemical pattern could hypothetically suggest an input of meteoric waters due to the exhumation and uplift of the region during late Cretaceous associated with Peruvian orogeny, and after the region had experienced a very low-grade metamorphism [37–39,55,56].

6. Conclusions

Carbonate mineralogy and composition was demonstrated as a useful method to distinguish between ore-related hydrothermal alteration and regional alteration. Thus, in Palai-Islica volcanic hosted epithermal deposit, calcite(±dolomite) is associated with regional alteration. Meanwhile, dolomite(±ankerite±siderite) is associated with the hydrothermal ore system. On the other hand, carbonates directly related to ore-forming processes and base-metal precipitation tend to show elevated Mn (and, to a lesser extent, Fe) contents. Thus, dolomite from the Palai-Islica deposit and local area shows this distinctive Mn average content: orebody veins (0.60 at. %) > hydrothermal alteration (0.44 at. %) > barren veins (0.16 at. %). Additionally, calcite from the La Serena area also shows an average Mn content clearly associated with its origin: "Chilean Manto-type" Cu(-Ag) (0.51 at. %) > metal rich Ag-Ba veins, (0.44 at. %) > metal poor Ag-Ba veins (0.12 at. %) > barren samples associated with very low-grade metamorphism (0.01 at. %). Instead, the Mg concentration in calcite is not directly correlated with ore-forming hydrothermal fluids but, maybe, with high-temperature, non-metal-rich fluids.

Carbonates from the mineralization typically show chemical zonation, although a unique pattern was not observed. In the two studied epithermal volcanic hosted deposits, subtle oscillatory patterns and more contrasting chemical zones were distinguished in dolomite/ankerite, reflecting a complex chemical evolution of the hydrothermal system. In "Chilean Manto-type" and Ag-Ba veins, dissolution textures in calcite are common, reflecting a late Mn(-Fe) stage, which could correspond with a stage dominated by oxidizing meteoric fluids. This similar zonation pattern among these two kinds of deposit also suggests a genetic link between both types of deposits.

The textural (space infillings) and chemical characterization (Mn, and very low Fe content) of the studied samples also showed two cases where calcite (stratabound Mn deposits of Quebrada Marquesa; low-grade disseminated mineral association from a "Chilean Manto-type" mineralization in Melipilla) is probably not related to the ore mineralization processes, perhaps reflecting the circulation of later meteoric waters post-mineralization. This conclusion should prevent us from using stable and radiogenic isotope analyses of these carbonates in the modeling of the primary genesis of these deposits.

In summary, the textures and chemical composition of carbonates provide an interesting and effective tool to fully constrain the likely origin of the carbonate phases and may help to discern or dismiss links between different styles of mineralization within a given area. It may be particularly useful prior to the application of stable and radiogenic isotope analyses of carbonate phases or simply as another tool in mineral exploration.

Supplementary Materials: The following are available online at www.mdpi.com/article/10.3390/min11080822/s1, Table S1: Summary of EPMA analysis of carbonates from epithermal Au-Cu deposits (Palai-Islica-SE Spain, and El Dorado-Central Chile) and host rock. Table S2: Summary of EPMA analysis of calcites from "Chilean Manto-type" Cu(-Ag) deposits (La Serena-Quebrada Marquesa- and Melipilla, Central Chile). Table S3: Summary of EPMA analysis of calcites from stratabound Mn and Ag-Ba vein deposits (Quebrada Marquesa and Arqueros -La Serena-, central Chile). Table S4: Summary of EPMA analysis of calcites from very low-grade metamorphism (La Serena and Melipilla, central Chile).

Author Contributions: Conceptualization, J.C.-R., S.M.-R. and D.M.; methodology, J.C.-R., S.M.-R. and M.B.; sampling and data collection, J.C.-R., S.M.-R., D.M. and M.B.; data analysis, J.C.-R., S.M.-R. and D.M.; interpretation data and discussion: J.C.-R., S.M.-R., D.M. and S.R.; writing—original draft preparation, J.C.-R., S.M.-R., D.M. and S.R.; writing—review and editing, J.C.-R., S.M.-R., S.R., D.M. and M.B, funding acquisition, J.C.-R. and S.M.-R. All authors have read and agreed to the published version of the manuscript.

Funding: The research was initially supported by the Spanish projects BTE-2003-06265 and CGL2006-02594-BTE (Ministry of Science and Technology/ Ministry of Science and Innovation/Ministry of Education and Science and FEDER), the RNM 131 of Junta de Andalucía, and the Chilean FONDECYT Project 1031000.

Institutional Review Board Statement: Not applicable.

Data Availability Statement: Not applicable.

Acknowledgments: We thank Fernando de la Fuente, Tsuyoshi Nishimura, Roberto Belmar, Alonso Toledo and Olga Veloso for their collaboration on this research and for their help to access to the studied mines and samples. The manuscript was significantly improved by the helpful suggestions and critiques of two anonymous reviewers. Assistant editor, Vivi Li, are also thanked for her help and encouragement.

Conflicts of Interest: The authors declare no conflict of interest.

References

1. Polgari, M.; Okita, P.M.; Hein, J.R. Stable isotope evidence for the origin of the Úrkút manganese ore deposit, Hungary. *J. Sed. Petrol.* **1991**, *61*, 384–393, doi:10.1306/D426771C-2B26-11D7-8648000102C1865D
2. Spangenberg, J.; Fontbote, L.; Sharp, Z.D.; Hunziker, J. Carbon and oxygen isotope study of hydrothermal carbonates in the zinc-lead deposits of the San Vicente district, central Peru: a quantitative modeling on mixing processes and CO_2 degassing. *Chem. Geol.* **1996**, *133*, 289–315, doi:10.1016/S0009-2541(96)00106-4
3. Bouzenoune, A.; Lecolle, P. Petrographic and geochemical arguments for hydrothermal formation of the Ouenza siderite deposit (NE Algeria). *Mineral. Deposita* **1997**, *32*, 189–196, doi:10.1007/s001260050084
4. Gianelli, G.; Ruggieri, G.; Mussi, M. Isotopic and fluid-inclusion study of hydrothermal and metamorphic carbonates in the Larderello geothermal field and surrounding areas, Italy. *Geothermics* **1997**, *26*, 393–417, doi:10.1016/S0375-6505(97)00001-1
5. Castorina, F.; Masi, U. Sr-isotopic composition of siderite for assessing the origin of mineralizing fluid: the case study from the Jebel Awam deposit (Central Morocco). *Ore Geol. Rev.* **2000**, *17*, 83–89, doi:10.1016/S0169-1368(00)00006-8
6. Wilkinson, J.J.; Earls, G. A high-temperature hydrothermal origin for black dolomite matrix breccias in the Irish Zn-Pb orefield. *Mineral. Mag.* **2000**, *64*, 1017–1036, doi:10.1180/002646100550029
7. Lavric, J.; Spangenberg, J. Stable isotope (C, O, S) systematics of the mercury mineralization at Idrija, Slovenia: constraints on fluid source and alteration processes. *Mineral. Deposita* **2003**, *38*, 886–899, doi:10.1007/s00126-003-0377-9
8. Wilkinson, J.J.; Everett, C.E.; Boyce, A.J.; Gleeson, S.A.; Rye, D.M. Intracratonic crustal seawater circulation and the genesis of subseafloor zinc-lead mineralization in the Irish orefield. *Geology* **2005**, *33*, 805–808, doi:10.1130/G21740.1
9. Schroll, E.; Koppel, V.; Cerny, I. Pb and Sr isotope and geochemical data from the Pb-Zn deposit Bleiberg (Austria): constraints on the age of mineralization. *Mineral. Petrol.* **2006,** *86*, 129–156, doi:10.1007/s00710-005-0107-3
10. Song, Y.; Hou, Z.; Cheng, Y.; Yang, T.; Xue, C. Fluid inclusion and isotopic constraints on the origin of ore-forming fluid of the Jinman–Liancheng vein Cu deposit in the Lanping Basin, western Yunnan, China. *Geofluids* **2016**, *16*, 56–77, doi:10.1111/gfl.12136

11. Marques de Sá, C.; Noronha, F.; Cardellach, E.; Bobos, I. Fluid inclusion and (S, C, O, Pb) isotope study of Pb-Zn-(Cu-Ag) hydrothermal veins from Central and Northern Portugal – Metallogenic implications. *Ore Geol. Rev.* **2019**, *112*, 1–15, doi:10.1016/j.oregeorev.2019.103043
12. Moroni, M.; Rossetti, P.; Naitza, S.; Magnani, L.; Ruggieri, G.; Aquino, A.; Tartarotti, P.; Franklin, A.; Ferrari, E.; Castelli, D.; Oggiano, G.; Secchi, F. Factors controlling hydrothermal nickel and cobalt mineralization—Some suggestions from historical ore deposits in Italy. *Minerals* **2019**, *9*, 429, doi:10.3390/min9070429
13. Maghfouri, S.; Hosseinzadeh, M.R.; Lentz, D.R.; Tajeddin, H.A.; Movahednia, M.; Shariefi, A. Nature of ore-forming fluids in the Mehdiabad world-class sub-seafloor replacement SEDEX-type Zn-Pb-Ba-(Cu-Ag) deposit, Iran; constraints from geochemistry, fluid inclusions, and O-C-Sr isotopes. *J. Asian Earth Sci.* **2021**, *207*, 104654, doi:10.1016/j.jseaes.2020.104654
14. Frondel, C. *The minerals of Franklin and Sterling Hill, a checklist*, John Wiley & Sons: New York, USA, **1972**; 94 pp.
15. Jebrak, M. Le district filonien a Pb-Zn-Ag et carbonates du Jebel Aouam (Maroc central). *Bull. Mineral.* **1985**, *108*, 487–498.
16. Polgari, M.; Forizs, I. Distribution of Mn in carbonates from the Upony Mts., NE-Hungary. *Geologica Carpathica* **1996**, *47*, 215–225.
17. Akçay, M.; Özkan, H.M.; Spiro, B.; Wilson, R.; Hoskin, P.W.O. Geochemistry of a high-T hydrothermal dolostone from the Emirli (Ödemis, western Turkey) Sb-Au deposit. *Mineral. Mag.* **2003**, *67*, 671–688, doi:10.1180/0026461036740126
18. Russell, M.J. Manganese halo surrounding the Tynagh ore deposit, Ireland: a preliminary note. *Trans. Inst. Min. Metall.* **1974**, *83*, B 65-66.
19. Gwosdz, W.; Krebs, W. Manganese halo surrounding Meggan ore deposit, Germany. *Trans. Inst. Min. Metall.* **1977**, *86*, B73 – B77.
20. Cruset, D.; Cantarero, I.; Vergés, J.; John, C. M.; Muñoz-López, D.; Travé, A. Changes in fluid regime in syn-orogenic sediments during the growth of the south Pyrenean fold and thrust belt. *Glob. Planet. Change* **2018**, *171*, 207–224, doi:10.1016/j.gloplacha.2017.11.001
21. Motte, G.; Hoareau, G.; Callot, J.-P.; Révillon, S.; Piccoli, F.; Calassou, S.; Gaucher, E. C. Rift and salt-related multi-phase dolomitization: example from the northwestern Pyrenees. *Mar. Pet. Geol.*, **2021**, 126, 104932, doi:10.1016/j.marpetgeo.2021.104932
22. Cruset, D.; Ibáñez-Insa, J.; Cantarero, I.; John, C. M.; Travé, A. Significance of fracture-filling rose-like calcite crystal clusters in the SE pyrenees. *Minerals* **2020**, *10*, 522, doi:10.3390/min10060522
23. Morales Ruano, S.; Carrillo Rosúa, F.J.; Fenoll Hach-Alí, P.; de la Fuente Chacón, F.; Contreras López, E. Epithermal Cu-Au mineralization in the Palai-Islica deposit, Almería, southeastern Spain: fluid inclusion evidence of mixing of fluids as guide to gold mineralization. *Can. Mineral.* **2000**, *38*, 553–566, doi:10.2113/gscanmin.38.3.553
24. Carrillo-Rosúa, F.J.; Morales-Ruano, S.; Fenoll Hach-Ali, P. Iron sulphides at the epithermal gold-copper deposit of Palai-Islica (Almería, SE Spain). *Mineral. Mag.* **2003**, *67*, 1059–1080, doi:10.1180/0026461036750143
25. Carrillo-Rosúa, F.J.; Morales Ruano, S.; Morata Céspedes, D. Mineral features of Cu-Ag-Ba-Mn mineralisations of La Serena, Chile. In *Mineral exploration and sustainable development*; Eliopoulos, D.G. et al. Eds.; Millpress: Rotterdam, Netherlands, **2003**; Volume 2, pp. 953–956.
26. Carrillo-Rosúa, J.; Morales-Ruano, S.; Fenoll Hach-Alí, P. Textural and chemical features of sphalerite from the Palai-Islica deposit (SE Spain): implications for ore genesis and color. *N. Jb. Miner. Abh.* **2008**, *185*, 63–78, doi:10.1127/0077-7757/2008/0109
27. Carrillo-Rosúa, J.; Morales-Ruano, S.; Esteban-Arispe, I.; Fenoll Hach-Alí, P. Significance of phyllosilicate mineralogy and mineral chemistry in an epithermal environment. Insights from the Palai-Islica Au-Cu deposit (Almería, SE Spain). *Clays Clay. Miner.* **2009**, *57*, 1–24, doi:10.1346/CCMN.2009.0570101
28. Carrillo-Rosúa, J. El depósito epitermal de oro-cobre Palai-Islica (Carboneras, Almería). Mineralogía, geoquímica y metalogenia. Unpublished PhD thsis. **2005**, 421 pp.
29. Carrillo-Rosúa, J.; Morales-Ruano, S.; Morata, D.; Boyce, A.J.; Belmar, M.; Fallick, A.E.; Fenoll Hach-Alí, P. Mineralogy and geochemistry of El Dorado epithermal gold deposit, El Sauce district, central-northern Chile. *Miner. Petrol.* **2008**, *92*, 341–360, doi:10.1007/s00710-007-0203-7
30. Boric, R. Geología y yacimientos metálicos del Distrito Talcuna, Región de Coquimbo. *Rev. Geol. Chile* **1985**, *25-26*, 57-75.
31. Oyarzun, R.; Ortega, L.; Sierra, J.; Lunar, R.; Oyarzun, J. Cu, Mn and Ag mineralization in the Quebrada Marquesa Quadrangle: the Talcuna and Arqueros district. *Mineral. Deposita* **1998**, *33*, 547–559, doi:10.1007/s001260050171
32. Carrillo-Rosúa, F.J.; Morales Ruano, S.; Morata, D.; Belmar, M.; Fenoll Hach-Alí, P. Fluidos relacionados con diferentes mineralizaciones de Cu-Ag y metamorfismo de bajo grado en el área de la Serena (Cordillera de la Costa, Chile Central). Datos preliminares. *Macla* **2004**, *2*, 89–90.
33. Carrillo-Rosúa, J.; Boyce, A.J.; Morales-Ruano, S.; Morata, D.; Roberts, S.; Munizaga, F.; Moreno-Rodríguez, V. Extremely negative and inhomogeneous sulfur isotope signatures in Cretaceous Chilean manto-type Cu–(Ag) deposits, Coastal Range of central Chile. *Ore Geol. Rev.* **2014**, *56*, 13–24, doi:10.1016/j.oregeorev.2013.06.013
34. Turner, S.P.; Platt, J.P.; George, R.M.M.; Kelley, S.P.; Pearson, D.G.; Nowell, G.M. Magmatism associated with orogenic collapse of the Betic-Alboran domain, SE Spain. *J. Petrol.* **1999**, *40*, 1011–1036, doi:10.1093/petroj/40.6.1011
35. Carrillo-Rosúa, F.J.; Morales Ruano, S.; Fenoll Hach-Alí, P. The three generations of gold in the Palai-Islica epithermal deposit, southeastern Spain. *Can. Mineral.* **2002**, *40*, 1465–1481, doi:10.2113/gscanmin.40.5.1465
36. Aguirre, L.; Egert, E. Cuadrángulo Quebrada Marquesa, provincia de Coquimbo. *Carta Geológica de Chile, Instituto de Investigaciones Geológicas* **1965**, *15*, 92 pp.

37. Morata, D.; Féraud, G.; Aguirre, L.; Arancibia, G.; Belmar, M.; Morales, S.; Carrillo, J. Geochronology of the lower cretaceous volcanism from the Coastal Range (29°20′-30°S), Chile. *Rev. Geol. Chile* **2008**, *35*, 123–145, doi:10.4067/S0716-02082008000100006
38. Morata, D.; Aguirre, L. Extensional Lower Cretaceous volcanism in the Costal Range (29º20′ - 30º00′ S) Chile: geochemistry and petrogenesis. *J. S. Amer. Earth Scien.* **2003**, *16*, 459–476, doi:10.1016/j.jsames.2003.06.001
39. Morata, D.; Aguirre, L.; Belmar, M.; Morales, S. Constraining very low-grade metamorphic conditions based on prehnite chemistry. Volumen de Abstract del 10º Congreso Geológico Chileno, Concepción, Chile, 6-10 octubre 2003; Sociedad Geológica de Chile, Chile, **2003**; 33–37.
40. Rutter, E. H.; Faulkner, D. R.; Burgess, R. Structure and geological history of the Carboneras Fault Zone, SE Spain: Part of a stretching transform fault system. *J. Struct. Geol.*, **2012**. 45, 68–71, doi:10.1016/j.jsg.2012.08.009
41. Abad, I.; Jiménez-Millán, J.; Schleicher, A. M.; van der Pluijm, B. A. Mineral characterization, clay quantification and Ar-Ar dating of faulted schists in the Carboneras and Palomares Faults (Betic Cordillera, SE Spain). *Eur. J. Mineral.*, **2017**, *29*, 17–34, doi:10.1127/ejm/2017/0029-2580
42. Bellon, H.; Bordet, P.; Montenat, C. Chronologie du magmatisme Néogène des Cordillères Bètiques (Espagne mèridionale). *Bull. Soc. Geol. Fr.* **1983**, *25*, 205–217.
43. Rosenberg, P.E.; Holland, H.D. Calcite-dolomite magnesite stability relations in solutions at elevated temperatures. *Science* **1964**, *145*, 700–701, doi:10.1126/science.145.3633.700
44. Garrels, R.M.; Thompson, M.E. A chemical model for sea water at 25°C and one atm. total pressure. *Amer. J. Sci.* **1962**, *260*, 57–66.
45. Fernández Soler, J.M. *El vulcanismo calco-alcalino en el Parque Natural de Cabo de Gata-Nijar (Almería). Estudio volcanológico y petrológico* Ph.D. thesis, University of Granada, Granada, Spain; Soc. Almeriense Historia Natural: Spain, **1996**; 295 pp.
46. Rimstidt, J.D.; Balog, A.; Webb, J. Distribution of carbonate minerals and aqueous solutions. *Geochim. Cosmochim. Acta* **1998**, *62*, 1851–1863, doi:10.1016/S0016-7037(98)00125-2
47. Anovitz, L. M.; Essene, E. J. Phase Equilibria in the System CaCO3-MgCO3-FeCO3. *J Petrol.* **1987**, *28*, 389–415, doi:10.1093/petrology/28.2.389
48. Heald, P.; Foley, N.K.; Hayba, D.O. Comparative anatomy of volcanic-hosted epithermal deposits; acid-sulfate and adularia-sericite types. *Econ. Geol.* **1987,** *82*, 1–26, doi:10.2113/gsecongeo.82.1.1
49. Hedenquist, J.W.; Arribas. A.; Gonzalez-Urien, E. Exploration for epithermal gold deposits. In *Gold in 2000;* Hagemann, S.G., Brown, P.E., Eds.; Society of Economic Geologists: CO, USA, **2000**; *Rev. Econ. Geol.*, review 13, pp. 245–277.
50. Wang, Y.; Xu, H. Prediction of trace metal partitioning between minerals and aqueous solutions: A linear free energy correlation approach. *Geochim. Cosmochim. Acta* **2001**, *65*(10), 1529–1543, doi:10.1016/S0016-7037(01)00551-8
51. Böttcher, M. E.; Dietzel, M. Metal-ion partitioning during low-temperature precipitation and dissolution of anhydrous carbonates and sulphates. *Eur. Mineral. Union Notes Mine*. **2010**, *10*, doi:10.1180/EMU-notes.10.4
52. Scott, S.D. Submarine hydrothermal systems and deposits. In *Geochemistry of hydrothermal ore deposits,* 3rd ed.; Barnes, H.L. Ed.; John Wiley & Sons: NY, USA, **1997**; pp. 435-486.
53. Yardley, B.W.D. Metal concentrations in crustal fluids and their relationship to ore formation. *Econ. Geol.* **2005**, *100*, 613–632, doi:10.2113/gsecongeo.100.4.613
54. McKibben, M.A.; Hardie, L.A. Ore-forming brines in active continental rifts. In *Geochemistry of hydrothermal ore deposits,* 3rd ed.; Barnes, H.L., Ed.; John Wiley & Sons: NY, USA, **1997**; pp. 877–935.
55. Charrier, R.; Ramos, V. A.; Tapia, F.; Sagripanti, L. Tectono-stratigraphic evolution of the Andean Orogen between 31 and 37°S (Chile and Western Argentina). *Geol. Soc. Spec. Publ.* **2015**. *399*, doi:10.1144/SP399.20
56. Wilson, N.S.F.; Zentilli, M.; Reynolds, P. H.; Boric, R.; Age of mineralization by basinal fluids at the El Soldado manto-type copper deposit, Chile: $^{40}Ar/^{39}Ar$ geochronology of K-feldspar. *Chem. Geol*. **2003**, *197*, 161–176.